

Math Modeling to Analyze the Health of the Gut Microbiome

by

Margaret Lorraine Cathcart

A thesis submitted to the Graduate Faculty of
Auburn University
in partial fulfillment of the
requirements for the Degree of
Master of Science

Auburn, Alabama
May 2, 2026

Keywords: Mathematical Modeling, Gut Microbiome, Ordinary Differential Equations

Copyright 2026 by Margaret Lorraine Cathcart

Approved by

Xiaoying Han, Chair, Professor of Mathematics
Hans-Werner Van Wyk, Associate Professor of Mathematics
Yuming Paul Zhang, Assistant Professor of Mathematics

Abstract

Understanding the gut microbiome and its link to human health is an important and marketable topic in modern science. Because of the difficulties related to directly examining and testing human guts, we turn to mathematical modeling. We use an Ordinary Differential Equations (ODE) model and the Monod growth form to model several functional groups and important products of fermentation. We modify an existing metabolite-explicit model [1], adding a hydrogen term and modeling its interactions with the existing microbes. We compare constant glucose inflow with three types of time-dependent glucose inflow. We conclude that glucose input is an indispensable aspect of this model, and its modulation can have substantial effects on each microbe.

Artificial Intelligence (AI) Use Disclosure Statement

In the preparation of this thesis, the following Artificial Intelligence (AI) tool was used: Google AI (powered by Gemini). This tool was used primarily to generate and debug Python code, and to find academic sources for literature review. The author acknowledges full responsibility for the intellectual content of this work. All AI-generated content was reviewed and validated for relevance, appropriateness, and accuracy before incorporation into the final document to maintain scholarly integrity of this research.

Digital Accessibility Disclosure Statement

In the preparation of this thesis, the following digital accessibility tools were used to ensure this document complies with federal requirements: Latex Compiler LuaLaTeX. The author acknowledges full responsibility for the intellectual content of this work and has made a good faith effort to comply with digital accessibility requirements in publishing, wherein the nature of the content does not significantly change in order to do so. Furthermore, all content has been reviewed and revised to meet these requirements prior to final publication.

Acknowledgments

I would first like to acknowledge that I could not achieve anything on my own. Everything I have, I credit to the Lord Jesus Christ.

As each has received a gift, use it to serve one another, as good stewards of God's varied grace: whoever speaks, as one who speaks oracles of God; whoever serves, as one who serves by the strength that God supplies—in order that in everything God may be glorified through Jesus Christ. To him belong glory and dominion forever and ever. Amen. - 1 Peter 4:10-11 (ESV)

I would like to thank my advisor, Dr. Xiaoying Han, for her consistent support and insightful guidance during the research and writing process. Without her passion and leadership, none of this work would have come to fruition. Additionally, to my committee members, Dr. Van Wyk and Dr. Zhang, thank you for your time and support.

To my family - Mom, Dad, Robert and Campbell, Sally, Charlie, and Sarah Campbell—thank you for answering all of my phone calls in the last two years. Soon I will show up at your door rather than calling you on the phone!

Thank you to my first mathematics professor, Dr. Daniel Savu, who encouraged me to pursue a math degree. To Dr. Brown, thank you for your wisdom and passion for Algebra. And finally, Dr. Lanius, I am so grateful for your cheerful and encouraging presence!

Table of Contents

Abstract	ii
Artificial Intelligence (AI) Use Disclosure Statement	iii
Digital Accessibility Disclosure Statement	iv
Acknowledgments	v
List of Tables	viii
List of Figures	ix
1 Introduction	1
1.1 The Gut Microbiome	1
1.2 Factors that Affect the Gut Microbiome	1
1.3 Colon Health	2
1.4 The Gut-Brain Axis	3
1.5 Fermentation	4
1.6 Mathematical Modeling for the Gut Microbiome	5
1.7 Notable Models	5
2 The Microbes in the Colon	8
2.1 Carbohydrates	8
2.2 Butyrate	8
2.3 Acetogen	9
2.4 Glucose	9
2.5 Acetate	9
2.6 Formate	10
2.7 Carbon Dioxide (CO_2)	10
2.8 Hydrogen Gas (H_2)	10

3	The Model	11
3.1	Approaches of Microbiome Modeling	11
3.2	The Metabolite-Explicit Model	12
3.3	The Revised Model with added H_2	15
3.4	Alternative Glucose Inflow Approaches	18
3.4.1	Periodic G_{in}	18
3.4.2	Average G_{in}	19
3.4.3	Piecewise G_{in}	20
3.4.4	Comparison of G_{in} Modeling Methods	21
3.5	Equilibrium Points	23
4	Discussion and Conclusions	27

List of Tables

3.1	Relationships between Functional Groups	14
3.2	Parameters used in the Rios Garza model. i is the actor, j is the substrate. . .	15
3.3	Relationships between Functional Groups with Hydrogen added.	16

List of Figures

- 3.1 The Rios Garza Model. Parameter Values: $\phi = .8, \mu_{max1} = .9, \mu_{max2} = .7, \mu_{max3} = .9, K_{11} = .6, K_{21} = .8, K_{22} = 1, K_{31} = 1, K_{33} = 1, K_{34} = 1, w_{22} = 1, w_{33} = 1, w_{34} = 1, G_{in} = 9, Y_{11} = 1, Y_{21} = .9, Y_{31} = .7, Y_{22} = .9, Y_{33} = 1, Y_{34} = 1, \alpha_{12} = .5, \alpha_{32} = 1, \alpha_{13} = .7, \alpha_{24} = .9$ 15
- 3.2 Rios Garza model with added H_2 Parameter Values: $\phi = .83, \mu_{max1} = .9, \mu_{max2} = .7, \mu_{max3} = .92, K_{11} = .81, K_{21} = .79, K_{22} = .8, K_{31} = .12, K_{33} = .1, K_{34} = 1, K_{25} = 1, K_{35} = .6, w_{22} = .2, w_{33} = .9, w_{34} = .2, w_{25} = .35, w_{35} = .05, G_{in} = 15, Y_{11} = .9, Y_{21} = .7, Y_{31} = .002, Y_{22} = .9, Y_{33} = 1, Y_{34} = .1, Y_{35} = .01, Y_{25} = .15, \alpha_{12} = .9, \alpha_{32} = .6, \alpha_{13} = .99, \alpha_{24} = .7, \alpha_{15} = .9$ 18
- 3.3 Periodic G_{in} term plots. Note that these are the same parameters used in Table 3.2. Parameter Values: $\phi = .83, \mu_{max1} = .9, \mu_{max2} = .7, \mu_{max3} = .92, K_{11} = .81, K_{21} = .79, K_{22} = .8, K_{31} = .12, K_{33} = .1, K_{34} = 1, K_{25} = 1, K_{35} = .6, w_{22} = .2, w_{33} = .9, w_{34} = .2, w_{25} = .35, w_{35} = .05, G_{in} = 15, Y_{11} = .9, Y_{21} = .7, Y_{31} = .002, Y_{22} = .9, Y_{33} = 1, Y_{34} = .1, Y_{35} = .01, Y_{25} = .15, \alpha_{12} = .9, \alpha_{32} = .6, \alpha_{13} = .99, \alpha_{24} = .7, \alpha_{15} = .9, w = .2, \lambda_1 = 0, \lambda_2 = 50$ 19
- 3.4 Average G_{in} term plots. Note that these are the same parameters used in Table 3.2. Parameter Values: $\phi = .83, \mu_{max1} = .9, \mu_{max2} = .7, \mu_{max3} = .92, K_{11} = .81, K_{21} = .79, K_{22} = .8, K_{31} = .12, K_{33} = .1, K_{34} = 1, K_{25} = 1, K_{35} = .6, w_{22} = .2, w_{33} = .9, w_{34} = .2, w_{25} = .35, w_{35} = .05, G_{in} = 15, Y_{11} = .9, Y_{21} = .7, Y_{31} = .002, Y_{22} = .9, Y_{33} = 1, Y_{34} = .1, Y_{35} = .01, Y_{25} = .15, \alpha_{12} = .9, \alpha_{32} = .6, \alpha_{13} = .99, \alpha_{24} = .7, \alpha_{15} = .9, w = .2, \lambda_1 = 0, \lambda_2 = 50, T = 500$ 20

3.5 Piecewise G_{in} term plots. Parameter Values: $\phi = .3, \mu_{max1} = .9, \mu_{max2} = .9, \mu_{max3} = .9, K_{11} = .6, K_{21} = .8, K_{22} = .5, K_{31} = .1, K_{33} = .1, K_{34} = 1, K_{25} = 1, K_{35} = .6, w_{22} = .2, w_{33} = .9, w_{34} = .2, w_{25} = .35, w_{35} = .05, L = 3, Y_{11} = 1, Y_{21} = .9, Y_{31} = .7, Y_{22} = .9, Y_{33} = 1, Y_{34} = .1, Y_{35} = .5, Y_{25} = 1, \alpha_{12} = .5, \alpha_{32} = 1, \alpha_{13} = .99, \alpha_{24} = .9, \alpha_{15} = .6, T = 500, n = 50. \dots \dots \dots 21$

3.6 The Biomass of Butyrate Producer using all four Glucose Inflow Approaches. Parameter Values: $\phi = .6, \mu_{max1} = .8, \mu_{max2} = .6, \mu_{max3} = .92, K_{11} = .81, K_{21} = .79, K_{22} = .8, K_{31} = .12, K_{33} = .1, K_{34} = .7, K_{25} = 1, K_{35} = .6, w_{22} = .3, w_{33} = .9, w_{34} = .2, w_{25} = .35, w_{35} = .05, G_{in} = L = 20, Y_{11} = .9, Y_{21} = .7, Y_{31} = .12, Y_{22} = .9, Y_{33} = .2, Y_{34} = 1, Y_{35} = .01, Y_{25} = .15, \alpha_{12} = .9, \alpha_{32} = .6, \alpha_{13} = .6, \alpha_{24} = .7, \alpha_{15} = .9, w = 2, \lambda_1 = \pi, \lambda_2 = 20, T = 150, n = 15. \dots \dots \dots 22$

3.7 The Biomass of H_2 using all four Glucose Inflow approaches. Parameter values: $\phi = .6, \mu_{max1} = .8, \mu_{max2} = .5, \mu_{max3} = .92, K_{11} = .81, K_{21} = .79, K_{22} = .8, K_{31} = .12, K_{33} = .1, K_{34} = .7, K_{25} = 1, K_{35} = .6, w_{22} = .3, w_{33} = .9, w_{34} = .2, w_{25} = .35, w_{35} = .05, G_{in} = L = 20, Y_{11} = .9, Y_{21} = .7, Y_{31} = .12, Y_{22} = .9, Y_{33} = .2, Y_{34} = .1, Y_{35} = .01, Y_{25} = .15, \alpha_{12} = .9, \alpha_{32} = .6, \alpha_{13} = .6, \alpha_{24} = .7, \alpha_{15} = .9, w = 2, \lambda_1 = \pi, \lambda_2 = 20, T = 150, n = 15. \dots \dots \dots 22$

Chapter 1

Introduction

1.1 The Gut Microbiome

One of the most popular health topics in recent years has been the link between the gut microbiome and human health. Because of this boom, the commercial probiotic market is worth approximately 54 billion US Dollars worldwide [2]. Understanding the human gut microbiome is one of the most important tasks in the twenty-first century. Microbiomes are biological systems of varied communities of microorganisms that live in the same habitat and host, engaging in non-linear and dynamic interactions [3]. The gut microbiome is a collection of microorganisms that inhabit the human gastrointestinal tract, which is estimated to be colonized by over 10^{14} bacteria [4, 5]. The gastrointestinal (GI) tract is the collection of organs involved in converting food into energy sources while removing additional waste products. Digestion primarily happens in the upper gastrointestinal tract, while final nutrient extraction and fecal preparation occurs in the lower gastrointestinal tract. The main organ of the lower GI tract is the colon [6]. The colon is often divided into three regions; the proximal, transverse, and distal sections [7].

1.2 Factors that Affect the Gut Microbiome

There are numerous factors that can affect gut microbiome makeup, such as **age, diet, antibiotics, disease, and geographic location**. Age is a crucial factor in microbiome composition. Elderly individuals have unstable compositions, which can be altered by characteristics such as residence cohort and geographic location [8]. The microbiota of infants is extremely volatile, and varies based on gestational age, antibiotic use, feeding method, and

delivery method [8]. It can take infants who were delivered via C-Section up to two years to reach the same amount of bacteria like *Bifidiobacterium* as infants who were delivered naturally [9].

Generally, diet changes microbiota composition by affecting metabolic activity [8]. Actors in the food industry are invested in the effects of ingredients on the composition of the microbiota [10]. Antibiotic treatment generally leads to a decrease in microbiota diversity, but the microbiota typically returns to its pre-treatment state within a few days or weeks [8].

Disease plays a crucial role in gut health. Inflammatory Bowel Disease (IBD) is a term for a group of conditions caused by an abnormal response against the commensal microbiota in a susceptible host [11, 5]. Two diseases that fall under the category of IBD are Ulcerative Colitis (UC) and Crohn's Disease (CD). In UC patients, the disease is limited to the colon, while CD is an autoimmune disease where the immune system attacks the gastrointestinal tract, causing inflammation [11]. According to a study led by the Crohn's and Colitis foundation, nearly 1 in 100 Americans suffer from an IBD [12].

Another factor that affects microbiome makeup is geographic location. Winglee et al. tested urban and rural residents of the Hunan province in China and found that urbanization was associated with a loss of microbial diversity and an increase in gene diversity. The authors claimed that similar lifestyles to American populations lead to a loss of beneficial bacteria and an increase in potentially harmful genes [13].

1.3 Colon Health

More than 90% of the total microbial cells in the human body are located in the colon [10]. The contents of the gut are not directly accessible for testing and examination, so fecal matter is used to analyze changes in microbiome makeup [14]. Disruption to the microbiome have been associated with metabolic disease, cancer, and inflammatory bowel disease [5]. Imbalance of the microbial population in the gut is known as dysbiosis [15]. Many clinical

trials have attempted to harness the gut in prevention and treatment of diseases, including allergies, cancer, heart disease, and mental disease [16]. Thus, understanding how changes in the microbiome affect health is of the utmost importance.

Recently, prebiotics and probiotics have been used as a treatment method for some diseases [11]. Prebiotics are non digestible food ingredients that simulate growth and metabolic activity of certain microorganisms that are already present in the colon [14]. Most prebiotics are non-digestible carbohydrates, like resistant starch, and fructo- and lacto- oligosaccharides [17]. Probiotics are living non-pathogenic organisms used as food ingredients to benefit the hosts' health. Lactic acid bacteria, bifidiobacteria, and yeasts are used as probiotics [18]. Using prebiotics to change microbiota composition has been shown to promote SCFA production, which is associated with beneficial genera such as *Bifidobacterium* [19, 20].

The gut microbiome is also a target for making cancer treatments like chemotherapy and immunotherapy safer and more efficient [21]. Correction of the gut microbiome of obese subjects has been shown to protect against osteoarthritis, a degenerative disease that effects the joints [22]. Restoring healthy members of the gut microbiome has been suggested as an alleviation of risk for cardiovascular diseases and liver cirrhosis [23].

When considering the numerous organisms living in the gut, it is important to discuss which are harmful and which are beneficial to human health. Butyrate is thought to be important to impact the regulation of the immune system [10]. The fermentation products of carbohydrates are regarded as healthy [10] It is considered healthy to have more undigested carbohydrates than proteins in the colon [17]. Some undigested carbohydrates are also used as prebiotics [17]. Through fermentation, prebiotics create an acidic environment unfavorable for potentially pathogenic species like *Clostridium* and *e. coli* [14].

1.4 The Gut-Brain Axis

Another development that has brought attention to the gut microbiome is the exploration of the Gut-Brain Axis. The GI tract influences brain function, and brain function

can influence the GI tract [24]. Results of dysfunction in the gut-brain network are gut inflammation disorders, altered responses to acute and chronic stress, and altered behavior [24].

The Gut-Brain axis has been used to treat learning and memory disorders [25], shown to affect motor control and anxiety in mice [26], and used to treat nervous system disorders [9].

1.5 Fermentation

One of the main processes that occurs in the colon is fermentation. Fermentation is the anaerobic breakdown of carbohydrates and proteins by bacteria [27]. In fermentation, an actor transforms a substrate into an end product. A substrate is the substance affected by the action of the catalyst. Substrates can be used as nutrients or support [28]. Often, during fermentation, compounds other than the end product called byproducts are created. Substrates are used up during fermentation and are typically the limiting resource that keeps fermentation from happening indefinitely. In the colon, major end products are Short Chain Fatty Acids, gases, ammonia, phenol, amines and energy [27]. Fermented foods have the potential to impact gut microbiota by modifying levels of some compounds within food [29, 30].

Short Chain Fatty Acids (SCFAs) are considered the principal products of fermentation in the large intestine of man and other animals [27]. Short Chain Fatty Acids work as an energy source for colonic epithelial cells and help enhance gut barrier integrity [11]. The most common Short Chain Fatty Acids (SCFAs) in the colon are acetate, propionate, butyrate, lactate, and succinate. SCFAs stimulate mucus production. Mucus acts as an energy source for gut microbes [29]. Most gut bacteria can produce acetate, formate and lactate, while propionate and butyrate production is more restricted [31].

1.6 Mathematical Modeling for the Gut Microbiome

The gut microbiome is complex, with trillions of microbial cells taking residence inside of it. In order to understand such a diverse system, we turn to mathematical modeling. Mathematical modeling offers value because it integrates and compiles known information and can complement new experimental data [3]. Using modeling as a form of understanding a system can be inexpensive and convenient. Graph models, boolean models, constraint-based models, and differential equation models have all been used to understand the gut microbiome [3].

Adrian et al. argued that while using Ordinary Differential Equations (ODE) based modeling for large systems can become impractical, pairing ODE modeling with other types of modeling like agent-based modeling can lead to insights into microbial interactions in the gut [32]. Agent-based modeling is a distinct modeling framework, often performed through software [3]. Differential equations are useful because they track information over time and importance of parameters and stability are able to be analyzed [32]. Many ODE models use a reductionist approach, where a complex biological system is simplified using assumptions that reduce the number of parameters and variables [33]. Of course, it is impossible to create a model that accounts for every microbe in the gut. Kumar et al. acknowledged an urgent need for model and experimental-based reductionist studies [33]. The predictions and conclusions made by mathematical models are able to both confirm existing hypotheses and to create new ones.

1.7 Notable Models

In a 2013 paper, Kettle et al. modeled microbial dynamics in the colon using Monod Dynamics. They divided the bacteria into 10 bacterial functional groups (BFGs), simulating variation in human microbiota composition [34]. In 2022, Kettle et al. introduced a process-based model of the colon, dividing the colon into discrete compartments [7]. Smith et al. used

a tool called microPop:Colon which simulates the colon as a series of separate compartments, dividing it into regions or as a continuous model. The food itself was modeled over time and space during digestion. The base version of microPop uses Monod kinetics. The pH and substrate preferences of the Microbial Functional Groups are also included [35].

Labarthe et al. modeled the colon as a cylinder. They used convection-diffusion-reaction equations that govern the volume of intestinal mixture components and concentration of dissolved components [15].

Adrian et al. used the Monod form to model the growth of three important microorganism populations; *Bacteroides thetaiotaomicron*, *Methanobrevibacter smithii*, and *Eubacterium rectale*. The authors considered growth with respect to butyrate production. They modeled the human gut as a chemostat, a laboratory device where inflow and outflow can be controlled. They suggested that incorporating inflow and outflow terms is a natural way to represent the gut [32].

Shibasaki and Mitri used the generalized Lotka-Volterra (gLV) model, considering an upstream patch and a downstream patch of the gut. They concluded that upstream species with positive effects on downstream species can further increase downstream community stability [36].

Budithi et al. introduced a data driven ODE model of a certain colon cancer treatment called FOLFIRI (Folinic Acid, Fluorouracil, and Irinotecan). They focused on the the types of primary colon tumors based on patient's immune profiles [37].

Cremer et al. represented the density of Bacteroidetes using a Partial Differential Equations (PDE) model. They used a reaction-diffusion model and represent active mixing, convection and water uptake, and a Monod growth rate, which calculated the pH using the nutrient concentration [38].

Bucci and Xavier modeled the gut microbiome as a series of completely mixed wastewater reactors. They used pairwise Lotka-Volterra models to do this [39].

Fernandes and Kothare introduced a novel compartment model to simulate the gut-brain axis, representing the stomach in compartments while considering neuron activity. They used Michaelis-Menten growth (similar to Monod growth) with a Hill coefficient that accounts for nonlinear behavior [40].

Chapter 2

The Microbes in the Colon

2.1 Carbohydrates

Around 40 grams of carbohydrates, which consist of resistant starch, non-starch polysaccharides and oligosaccharides, reach the colon daily and are partially fermented by the gut microbiota [41]. Carbohydrates enter the colon mainly in the form of polysaccharides that either have not or cannot be hydrolyzed by host digestive enzymes in the small bowel [27]. Carbohydrates constitute 85% of the available substrates for colonic fermentation [42]. Carbohydrates are fermented by *bifidiobacteria* of the Phylum Actinobacteria. [18]. Products of carbohydrate fermentation are formate, acetate, lactate, and butyrate [31]. Carbohydrates are generally preferred by bacteria as a primary energy source if they are available [8].

2.2 Butyrate

Butyrate is a Short Chain Fatty Acid. Butyrate is crucial to maintain a healthy gut. It fuels enterocytes, signals to the host and is a mediator of colonic inflammatory response [43].

A small number of butyrate producers can grow on lactate. They have an important role in preventing the build-up of toxic lactate levels [31]. Butyrate producers are targeted by diseases like inflammatory bowel disease and diabetes [43]. Known butyrate producers belong to the *Clostridium* genus [43]. There is demand for studies that identify butyrate-producing bacteria [11].

2.3 Acetogen

Acetogens are an important functional group in the gut that are responsible for hydrogen removal through the production of acetate [43]. Acetogens are a varied group of microorganisms including bacteria from a diverse group of phyla.

Their most distinguishing feature is the ability to produce acetate from H_2 plus CO_2 [44]. Acetogens produce approximately one-third of the colonic acetate from hydrogen, carbon dioxide, or formic acid [45].

2.4 Glucose

Glucose is a simple sugar formed through hydrolysis of lactose [46]. Hydrolysis is the chemical reaction of a compound with water [28]. Often, glucose is used to represent carbohydrate substrates [47]. It is crucially important to the human body due to its richness in energy [44, 28].

Substrates are the materials used up during a process such as fermentation. Glucose is a soluble fiber. Primary fermenters, lactate consumers, acetogens, and methanogens all depend on glucose, and thus are competing for it [1].

2.5 Acetate

Acetate is a Short Chain Fatty Acid. Acetate is the most abundant SCFA in the colon and it makes up more than half of the total SCFA material detected in feces [45]. Many organisms produce acetate as an end product during carbohydrate fermentation [44].

Acetate acts as a substrate for cholesterol synthesis [32]. Acetate has been shown to modulate gut microbiota and reverse gut dysbiosis to some degree [29].

2.6 Formate

Formate is a common end product of fermentation, but, little is known about its role in the gut [29, 48]. Although the entire gut microbiome affects tumor growth during colorectal cancer, formate has been shown to drive colorectal cancer tumor invasion [49].

2.7 Carbon Dioxide (CO_2)

CO_2 is one of the major gases produced by colonic bacteria during fermentation of dietary substrates in the colon [46]. It is either a by-product or a an intermediate product that is formed through fermentation [46]. Unabsorbed CO_2 can be excreted in flatus or metabolized by resident microorganisms of the gut microbiome [46].

2.8 Hydrogen Gas (H_2)

Hydrogen gas is a common product of carbohydrate fermentation. As the most predominant gas produced by colonic bacteria, it is produced only by fermentation of non-digestible substrates in the colon [46]. Its accumulation can modulate fermentation.

A high concentration of H_2 can stimulate production of butyrate, an anti-inflammatory metabolite. If H_2 is consumed to create methane, it can decrease butyrate production [47]. Along with lactate, accumulation of hydrogen in the gut results in gastrointestinal disorders [43]. Because of this, microbes in the gut remove excess hydrogen. It is used by other microbes and passed as flatus or excreted through the breath [46].

Chapter 3

The Model

3.1 Approaches of Microbiome Modeling

A popular Differential Equations model for the microbiome is the Generalized Lotka-Volterra model (gLV) [3]. It handles changes in species abundance by balancing growth and pairwise stimulative or inhibitory interactions [3]. The gLV model depends upon interaction terms which are estimated by using community dynamics [4, 50].

Momeni et al. argued in their 2017 work that a single equation could not qualitatively capture diverse pairwise microbial interactions [50]. Microbes are competing for space and nutrients, and are controlled by microbial densities and resource concentrations [51]. Due to the complexity of microbial communities, it is difficult to express their relationships with a pairwise approach, which only considers two species at a time. Initiatives such as the Human Microbiome Project (HMP) were formed to find and catalog relationships between microbial inhabitants [52]. This data is used to determine the values of the interaction terms. Stein et al. extended the gLV model, adding an extra term that accounted for environmental variations. The authors used this variation term to infer microbiota ecology and predict temporal dynamics [53, 54]. Even with these developments, issues still arise with using the gLV form to model microbial dynamics. Thus, it is prudent to consider other options that incorporate multiple species interactions simultaneously to model the microbiome. One of these is the Monod form, which represents growth using the idea of actors and substrates. Although it is acknowledged as a stronger depiction of microbiome growth, criticisms of Monod growth still exist [1]. Some concerns are its basis on assumptions like fixed cell composition and saturation kinetics as well as the effort required to parameterise and simulate

the model [55]. Alternatives to mathematical modeling are artificially produced environment (in vitro) experiments, or in some cases human and animal (in vivo) experiments [56]. In vivo experiments are restricted and costly. Because of the difficulty and effort required to conduct these experiments, it is often prudent to use mathematical models instead of these other methods. To complicate the matter further, most microbes that are present in the microbiota are uncultivated in a lab setting [53]. Additionally, cost and repeatability, issues that are prevalent in in vitro and in vivo studies, are not a factor when using mathematical modeling. Models might not completely replace human trials, but they provide powerful tools for proof of concept studies before in vivo validation [57].

3.2 The Metabolite-Explicit Model

Rios Garza et al. presented a metabolite-explicit modeling approach as an alternative to the usual gLV model. They described the use of a kinetic model which focused on growth-limiting nutrients [1]. Rios Garza et al described relationships between microbes in four ways. They used the popular **Monod** function to represent growth with a single limiting substrate.

$$\mu = \mu_{max} \frac{S}{K_s + S}$$

μ is the growth an the organism. μ_{max} is the maximum specific growth rate, S is the concentration of the substrate, and K_s is the half saturation constant, which is the concentration of a substrate required in order for an actor to act at half of its maximum growth rate [28]. K_s measures the affinity of the actor for a certain substrate [28].

However, when several limiting substrates are present, kinetic models employ logic of nutrient use, which is acquired through experiments [1].

Obligate resources are resources that are simultaneously required for the growth of an organism. The growth rate is described as

$$\mu = \mu_{max} \frac{S_1}{K_1 + S_1} \frac{S_2}{K_2 + S_2}$$

Alternative resources are resources that can be replaced by one when the other is depleted. The growth rate is described as

$$\mu = \mu_{max} \left(w_1 \frac{S_1}{K_1 + S_1} + w_2 \frac{S_2}{K_2 + S_2} \right),$$

where the w_i terms are weights expressing nutrient contributions.

Boosting resources are resources where the presence of one nutrient can boost the growth of another. The growth rate is described as

$$\mu = \mu_{max} \frac{S_1}{K_1 + S_1} \left(w_1 + w_2 \frac{S_2}{K_2 + S_2} \right)$$

The **diauxic shift** introduces a threshold term K_s where the growth switches from growth on S_1 (when S_1 is high)to growth on S_2 (when S_1 is below K_s). The growth rate is described as

$$\mu = \mu_{max} \left(\frac{S_1}{K_1 + S_1} + w_s \frac{K_s^n}{K_s^n + S_1^n} \frac{S_2}{K_2 + S_2} \right)$$

In the model [1], actors of fermentation were represented as separate functional groups. For each substrate utilization, a certain microbial group catalyzed the conversion. Identifying and utilizing functional groups is a common approach for modeling ecological systems [42]. Rios Garza et al. chose a carbohydrate fermenter, an acetogen, and a butyrate producer for their functional groups. Each requires glucose and is thus competing for it. The relationships between the functional groups are described in Table 3.1.

Based on these relationships, the authors introduced this model,

Actor	End Product	Substrate	Boosting Resource
Carbohydrate Fermenter	Acetate and Formate and Glucose	Carbohydrates	
Acetogen	Acetate	Glucose (Alt. Formate, CO ₂)	
Butyrate Producer	Butyrate	Glucose	Acetate

Table 3.1: Relationships between Functional Groups

$$\begin{aligned}
\frac{dC}{dt} &= \mu_{max1} \frac{G}{K_{11} + G} C - \phi C \\
\frac{dB}{dt} &= \mu_{max2} \frac{G}{K_{21} + G} \left(1 + w_{22} \frac{E}{K_{22} + E} \right) B - \phi B \\
\frac{dA}{dt} &= \mu_{max3} \frac{G}{K_{31} + G} \left(w_{33} \frac{F}{K_{33} + F} + w_{34} \frac{CO_2}{K_{34} + CO_2} \right) A - \phi A
\end{aligned}$$

$$\begin{aligned}
\mu_1(G) &= \mu_{max1} \frac{G}{K_{11} + G} \\
\mu_2(G, E) &= \mu_{max2} \frac{G}{K_{21} + G} \left(1 + w_{22} \frac{E}{K_{22} + E} \right) \\
\mu_3(G, F, CO_2) &= \mu_{max3} \frac{G}{K_{31} + G} \left(w_{33} \frac{F}{K_{33} + F} + w_{34} \frac{CO_2}{K_{34} + CO_2} \right)
\end{aligned} \tag{3.1}$$

$$\begin{aligned}
\frac{dG}{dt} &= \phi G_{in} - \frac{\mu_1}{Y_{11}} C - \frac{\mu_2}{Y_{21}} B - \frac{\mu_3}{Y_{31}} A - \phi G \\
\frac{dE}{dt} &= \alpha_{12} \mu_1 C + \alpha_{32} \mu_3 A - \frac{\mu_{max2}}{Y_{22}} w_{22} \frac{G}{K_{21} + G} \frac{E}{K_{22} + E} B - \phi E \\
\frac{dF}{dt} &= \alpha_{13} \mu_1 C - \frac{\mu_{max3}}{Y_{33}} w_{33} \frac{G}{K_{31} + G} \frac{F}{K_{33} + F} A - \phi F \\
\frac{dCO_2}{dt} &= \alpha_{24} \mu_2 B - \frac{\mu_{max3}}{Y_{34}} w_{34} \frac{G}{K_{31} + G} \frac{CO_2}{K_{34} + CO_2} A - \phi CO_2
\end{aligned}$$

The parameters in Equation (3.1) are as follows.

Parameter	C	B	A	G	E	F	CO ₂
Meaning	Carbohydrate Fermenter	Butyrate Producer	Acetogen	Glucose	Acetate	Formate	Carbon Dioxide

Parameter	Meaning
ϕ	Flow Rate
μ_{maxj}	Maximum Growth Rate of j
Y_{ij}	Yield of i over j
α_{ij}	Production rate of i by j
K_{ij}	Half Saturation Constant of i and j
w_{ij}	Weight of j Contribution to i Growth
G_{in}	Concentration of Incoming Glucose

Table 3.2: Parameters used in the Rios Garza model. i is the actor, j is the substrate.

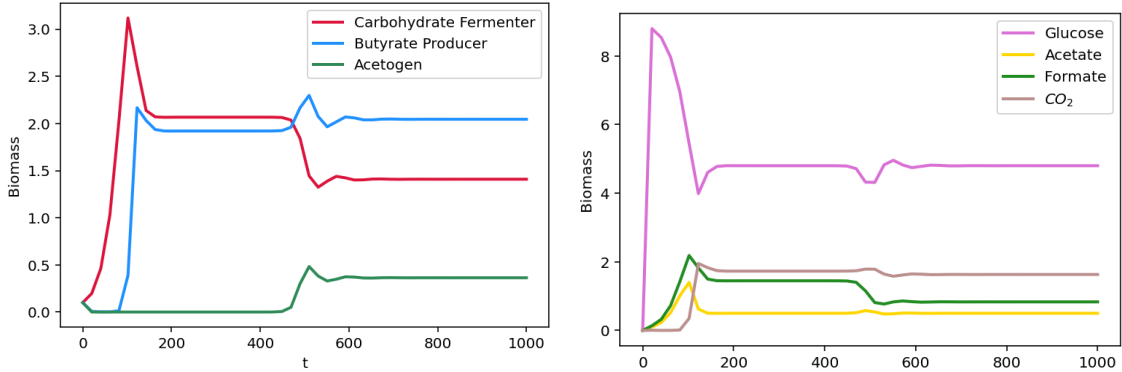


Figure 3.1: The Rios Garza Model. Parameter Values: $\phi = .8, \mu_{max1} = .9, \mu_{max2} = .7, \mu_{max3} = .9, K_{11} = .6, K_{21} = .8, K_{22} = 1, K_{31} = 1, K_{33} = 1, K_{34} = 1, w_{22} = 1, w_{33} = 1, w_{34} = 1, G_{in} = 9, Y_{11} = 1, Y_{21} = .9, Y_{31} = .7, Y_{22} = .9, Y_{33} = 1, Y_{34} = 1, \alpha_{12} = .5, \alpha_{32} = 1, \alpha_{13} = .7, \alpha_{24} = .9$

In Figure 3.1, the carbohydrate fermenter and butyrate producer parameters are higher than the acetogen, which is consistent with the high glucose content, as the carbohydrate producer depends on glucose alone in the model. The few dips and steadying effect of the functions is due to the constant glucose inflow term. Since all of the microbes depend on glucose, its constant inflow has a direct impact on each of their growth functions.

3.3 The Revised Model with added H_2

This model is an excellent beginning point to understand the Gut Microbiome. In this work, we are interested in considering more microbes that are relevant to fermentation. Hydrogen gas has been identified as an important driver in carbohydrate fermentation, which is a major aspect of this model [47, 35]. Because of its significance, we extend the model

Actor	End Product	Substrate	Boosting Resource
Carbohydrate Fermenter	Acetate, Formate and Hydrogen	Carbohydrates and Glucose	
Acetogen	Acetate	Glucose (Alternate: CO_2 , Formate, Hydrogen)	
Butyrate Producer	Butyrate	Glucose	Acetate, Hydrogen

Table 3.3: Relationships between Functional Groups with Hydrogen added.

to include hydrogen gas (H_2). The acetogen consumes hydrogen, so its growth rate includes Hydrogen. Additionally, the butyrate producer is boosted by hydrogen. The new dynamical system is described in Table 3.3.

Thus, the new model is

$$\begin{aligned}
\frac{dC}{dt} &= \mu_1(G)C - \phi C \\
\frac{dB}{dt} &= \mu_2(G, E, H_2)B - \phi B \\
\frac{dA}{dt} &= \mu_3(G, F, CO_2, H_2)A - \phi A \\
\mu_1 &= \mu_{max1} \frac{G}{K_{11} + G} \\
\mu_2 &= \mu_{max2} \frac{G}{K_{21} + G} \left(1 + w_{22} \frac{E}{K_{22} + E} + w_{25} \frac{H_2}{K_{25} + H_2} \right) \\
\mu_3 &= \mu_{max3} \frac{G}{K_{31} + G} \left(w_{33} \frac{F}{K_{33} + F} + w_{34} \frac{CO_2}{K_{34} + CO_2} + w_{35} \frac{H_2}{K_{35} + H_2} \right)
\end{aligned} \tag{3.2}$$

$$\begin{aligned}
\frac{dG}{dt} &= \phi G_{in} - \frac{\mu_1}{Y_{11}} C - \frac{\mu_2}{Y_{21}} B - \frac{\mu_3}{Y_{31}} A - \phi G \\
\frac{dE}{dt} &= \alpha_{12} \mu_1 C + \alpha_{32} \mu_3 A - \frac{\mu_{max2}}{Y_{22}} w_{22} \frac{G}{K_{21} + G} \frac{E}{K_{22} + E} B - \phi E \\
\frac{dF}{dt} &= \alpha_{13} \mu_1 C - \frac{\mu_{max3}}{Y_{33}} w_{33} \frac{G}{K_{31} + G} \frac{F}{K_{33} + F} A - \phi F \\
\frac{dCO_2}{dt} &= \alpha_{24} \mu_2 B - \frac{\mu_{max3}}{Y_{34}} w_{34} \frac{G}{K_{31} + G} \frac{CO_2}{K_{34} + CO_2} A - \phi CO_2 \\
\frac{dH_2}{dt} &= \alpha_{15} \mu_1 C - \frac{\mu_{max3}}{Y_{35}} w_{35} \frac{G}{K_{31} + G} \frac{H_2}{K_{35} + H_2} A \\
&\quad - \frac{\mu_{max2}}{Y_{25}} w_{25} \frac{G}{K_{21} + G} \frac{H_2}{K_{25} + H_2} B - \phi H_2
\end{aligned}$$

In Figure 3.2, we observe a coexistence state for all eight parameters. Glucose is the parameter with the highest biomass. Because it is necessary for each microbes' survival, it is necessary for glucose to exist at a higher rate than the other microbes. All of the parameters except for the acetogen appear to exhibit periodic behavior, but the up-and-down motion begins to lessen as time passes, particularly after $t = 1800$. This graphical behavior may be a sign that our solutions tend toward a limit cycle.

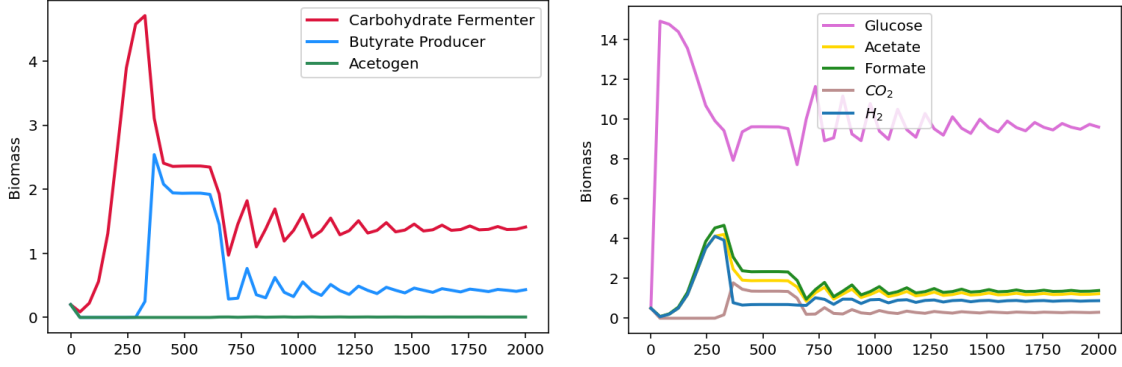


Figure 3.2: Rios Garza model with added H_2 Parameter Values: $\phi = .83, \mu_{max1} = .9, \mu_{max2} = .7, \mu_{max3} = .92, K_{11} = .81, K_{21} = .79, K_{22} = .8, K_{31} = .12, K_{33} = .1, K_{34} = 1, K_{25} = 1, K_{35} = .6, w_{22} = .2, w_{33} = .9, w_{34} = .2, w_{25} = .35, w_{35} = .05, G_{in} = 15, Y_{11} = .9, Y_{21} = .7, Y_{31} = .002, Y_{22} = .9, Y_{33} = 1, Y_{34} = .1, Y_{35} = .01, Y_{25} = .15, \alpha_{12} = .9, \alpha_{32} = .6, \alpha_{13} = .99, \alpha_{24} = .7, \alpha_{15} = .9$

3.4 Alternative Glucose Inflow Approaches

The existence of a constant G_{in} in this model has led to some complication when calculating numerical simulations. In particular, glucose persists when other microbes reach extinction, which does not correspond with our knowledge of the microbiome. In fact, glucose absorption peaks 30 to 40 minutes after a meal is ingested and peaks again 120 to 150 minutes after ingestion [58]. Therefore, we propose a few alternatives to a constant glucose inflow term that attempt to model such a phenomenon. The goal is to compare dynamical behavior of constant input to time dependent input with the same amount of glucose during a fixed period of time.

3.4.1 Periodic G_{in}

First, we propose a periodic G_{in} term. Then,

$$G_{in} = G(t) = \sin(\omega t + \lambda_1) + \lambda_2.$$

This periodic function may more accurately follow the glucose peaks discussed by Ferrannini [58].

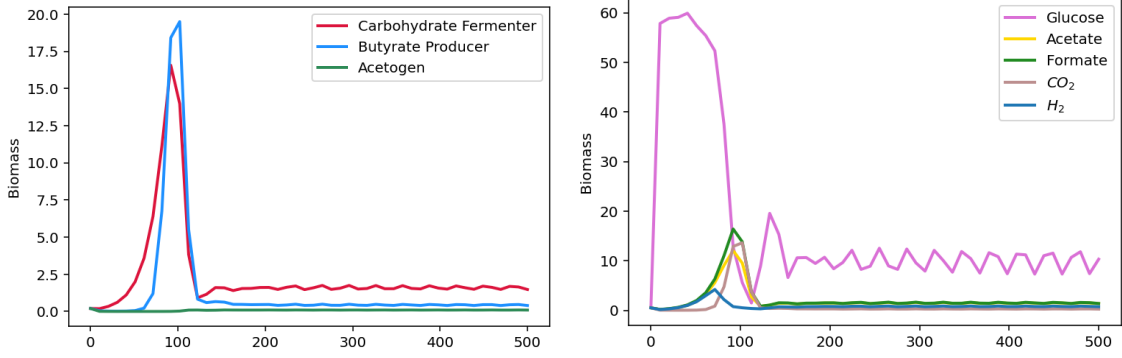


Figure 3.3: Periodic G_{in} term plots. Note that these are the same parameters used in Table 3.2. Parameter Values: $\phi = .83, \mu_{max1} = .9, \mu_{max2} = .7, \mu_{max3} = .92, K_{11} = .81, K_{21} = .79, K_{22} = .8, K_{31} = .12, K_{33} = .1, K_{34} = 1, K_{25} = 1, K_{35} = .6, w_{22} = .2, w_{33} = .9, w_{34} = .2, w_{25} = .35, w_{35} = .05, G_{in} = 15, Y_{11} = .9, Y_{21} = .7, Y_{31} = .002, Y_{22} = .9, Y_{33} = 1, Y_{34} = .1, Y_{35} = .01, Y_{25} = .15, \alpha_{12} = .9, \alpha_{32} = .6, \alpha_{13} = .99, \alpha_{24} = .7, \alpha_{15} = .9, w = .2, \lambda_1 = 0, \lambda_2 = 50$.

In Figure 3.3, because the parameter values are identical to those used in Figure 3.2 with the added vertical shift from λ_2 , the plots are remarkably similar. We can observe periodic behavior that persists over time, unlike the periodic looking behavior in Figure 3.2 that begins to taper into a straight line. The size of λ_2 is most likely responsible for the large peak at the beginning for the carbohydrate fermenter, butyrate producer, and glucose.

3.4.2 Average G_{in}

If we are evaluating the system over the timesteps $[0, T]$,

$$G_{in} = \frac{1}{T} \int_0^T (\sin(\omega t + \lambda_1) + \lambda_2) dt.$$

In Figure 3.4, we can observe similar graphical behavior to the Periodic G_{in} from Figure 3.3. Since the term is now an average, we see a much earlier halt of periodic looking behavior in comparison to Figure 3.2.

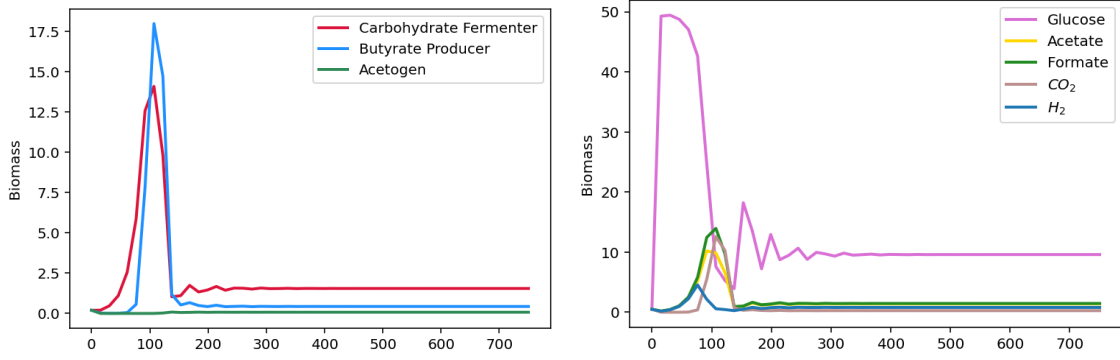


Figure 3.4: Average G_{in} term plots. Note that these are the same parameters used in Table 3.2. Parameter Values: $\phi = .83, \mu_{max1} = .9, \mu_{max2} = .7, \mu_{max3} = .92, K_{11} = .81, K_{21} = .79, K_{22} = .8, K_{31} = .12, K_{33} = .1, K_{34} = 1, K_{25} = 1, K_{35} = .6, w_{22} = .2, w_{33} = .9, w_{34} = .2, w_{25} = .35, w_{35} = .05, G_{in} = 15, Y_{11} = .9, Y_{21} = .7, Y_{31} = .002, Y_{22} = .9, Y_{33} = 1, Y_{34} = .1, Y_{35} = .01, Y_{25} = .15, \alpha_{12} = .9, \alpha_{32} = .6, \alpha_{13} = .99, \alpha_{24} = .7, \alpha_{15} = .9, w = .2, \lambda_1 = 0, \lambda_2 = 50, T = 500$.

3.4.3 Piecewise G_{in}

If we evaluate the system over the timesteps $[0, T]$, and we divide the function into n intervals, our G_{in} will be

$$G_{in} = \begin{cases} L & \text{if } t \in [k\frac{T}{n}, (k+1)\frac{T}{n}) \\ 0 & \text{if } t \in [(k+1)\frac{T}{n}, (k+2)\frac{T}{n}) \end{cases}$$

This works from 0 to q , where $k = 2q$, and $k = \frac{n}{2}$, and $n \geq 2$.

This type of inflow simulates a "stop-and-start" process that might better simulate how humans eat. Food inflow - and therefore glucose inflow - is not ordinarily constant in humans as meals are eaten at separate and distinct times of the day.

In Figure 3.5, we can observe how the piecewise G_{in} affects each microbe. Each microbe biomass hits a distinct peak and valley before spiking back up. Interestingly, at about $t = 250$, the glucose biomass peaks. As glucose peaks, the rest of the parameters seem to almost flatten, specifically the carbohydrate fermenter and butyrate producer. However, as

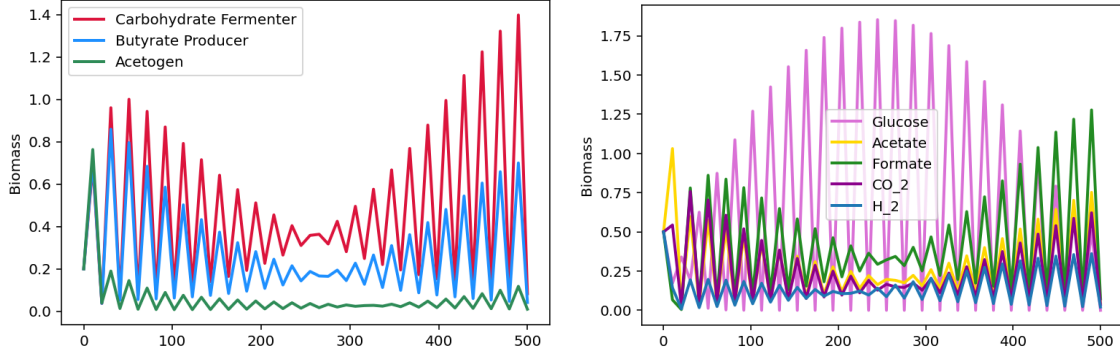


Figure 3.5: Piecewise G_{in} term plots. Parameter Values: $\phi = .3, \mu_{max1} = .9, \mu_{max2} = .9, \mu_{max3} = .9, K_{11} = .6, K_{21} = .8, K_{22} = .5, K_{31} = .1, K_{33} = .1, K_{34} = 1, K_{25} = 1, K_{35} = .6, w_{22} = .2, w_{33} = .9, w_{34} = .2, w_{25} = .35, w_{35} = .05, L = 3, Y_{11} = 1, Y_{21} = .9, Y_{31} = .7, Y_{22} = .9, Y_{33} = 1, Y_{34} = .1, Y_{35} = .5, Y_{25} = 1, \alpha_{12} = .5, \alpha_{32} = 1, \alpha_{13} = .99, \alpha_{24} = .9, \alpha_{15} = .6, T = 500, n = 50$.

glucose begins to decrease, all of the parameters increase until $t = 500$. This seems to imply that an overabundance of glucose leads to a decrease of all other biomasses.

3.4.4 Comparison of G_{in} Modeling Methods

In Figure 3.6, we can observe how the difference in Glucose Inflow result in drastic differences in the biomass of one parameter, the butyrate producer. The constant and average glucose inflow terms act similarly, while the periodic inflow term causes the butyrate producer to rise above the other versions. Because the piecewise G_{in} turns glucose inflow "off" at $t = 10$, the butyrate producer does not have a chance to recover from this loss and dies.

In Figure 3.7, we can observe the different Glucose Inflow terms impacting the biomass of H_2 . Much like Figure 3.6, the average and constant functions function in the same way. However, the periodic function yields in a higher biomass for H_2 than the other four terms, just like in Figure 3.6. The piecewise plot paints a picture of the different utility of the G_{in} term. The "on and off" nature of glucose is clearly impacting the H_2 term. At first, there is a noted increase after the valleys of glucose loss, but by $t = 120$, the biomass of H_2 begins to flatten.

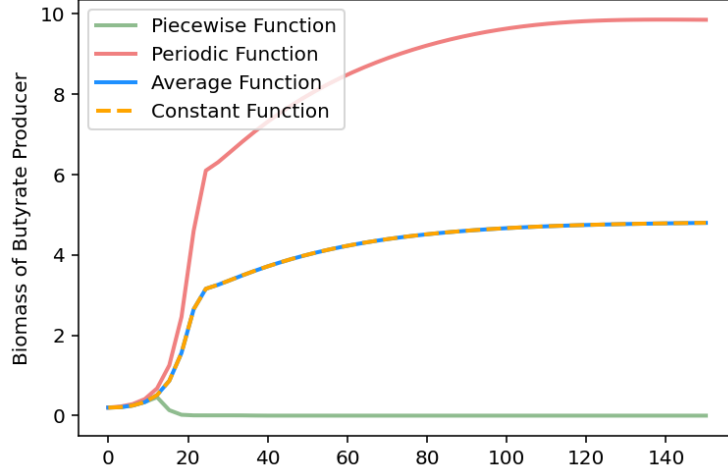


Figure 3.6: The Biomass of Butyrate Producer using all four Glucose Inflow Approaches. Parameter Values: $\phi = .6, \mu_{max1} = .8, \mu_{max2} = .6, \mu_{max3} = .92, K_{11} = .81, K_{21} = .79, K_{22} = .8, K_{31} = .12, K_{33} = .1, K_{34} = .7, K_{25} = 1, K_{35} = .6, w_{22} = .3, w_{33} = .9, w_{34} = .2, w_{25} = .35, w_{35} = .05, G_{in} = L = 20, Y_{11} = .9, Y_{21} = .7, Y_{31} = .12, Y_{22} = .9, Y_{33} = .2, Y_{34} = 1, Y_{35} = .01, Y_{25} = .15, \alpha_{12} = .9, \alpha_{32} = .6, \alpha_{13} = .6, \alpha_{24} = .7, \alpha_{15} = .9, w = 2, \lambda_1 = \pi, \lambda_2 = 20, T = 150, n = 15.$

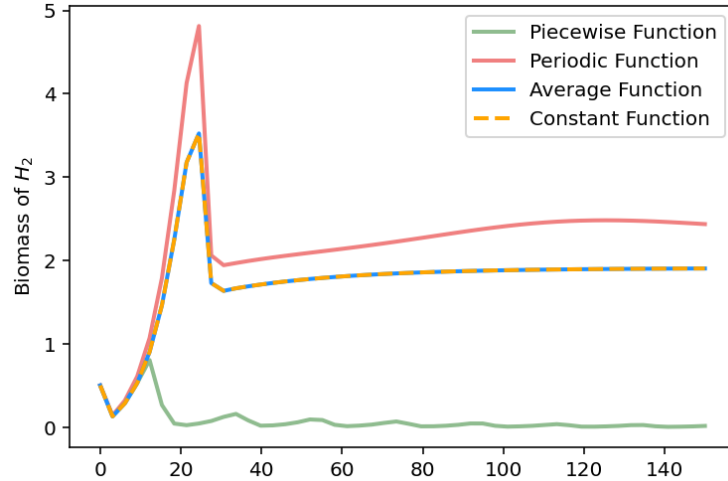


Figure 3.7: The Biomass of H_2 using all four Glucose Inflow approaches. Parameter values: $\phi = .6, \mu_{max1} = .8, \mu_{max2} = .5, \mu_{max3} = .92, K_{11} = .81, K_{21} = .79, K_{22} = .8, K_{31} = .12, K_{33} = .1, K_{34} = .7, K_{25} = 1, K_{35} = .6, w_{22} = .3, w_{33} = .9, w_{34} = .2, w_{25} = .35, w_{35} = .05, G_{in} = L = 20, Y_{11} = .9, Y_{21} = .7, Y_{31} = .12, Y_{22} = .9, Y_{33} = .2, Y_{34} = .1, Y_{35} = .01, Y_{25} = .15, \alpha_{12} = .9, \alpha_{32} = .6, \alpha_{13} = .6, \alpha_{24} = .7, \alpha_{15} = .9, w = 2, \lambda_1 = \pi, \lambda_2 = 20, T = 150, n = 15.$

3.5 Equilibrium Points

We consider the following non-negative equilibria:

1. $E_0 = (0, 0, 0, G_1^*, E_1^*, F_1^*, CO_{2(1)}^*, H_{2(1)}^*)$, where

$$\begin{aligned}\frac{dC}{dt} &= 0 \\ \frac{dB}{dt} &= 0 \\ \frac{dA}{dt} &= 0 \\ \frac{dG}{dt} &= \phi G_{in} - \phi G \\ \frac{dE}{dt} &= -\phi E \\ \frac{dF}{dt} &= -\phi F \\ \frac{dCO_2}{dt} &= -\phi CO_2 \\ \frac{dH_2}{dt} &= -\phi H_2\end{aligned}$$

Setting each expression equal to zero, we get that

$G = G_{in}, E = 0, F = 0, CO_2 = 0, H_2 = 0$. Therefore, our set of equilibrium points will be

$$(0, 0, 0, G_{in}, 0, 0, 0, 0).$$

Therefore, when there are no Functional Groups, only glucose persists at the population it is when it enters. Glucose is not being consumed when the fermentation process ends. This is why it is important to consider different G_{in} options.

2. $E_2 = (C_2^*, 0, 0, G_2^*, E_2^*, F_2^*, CO_{2(2)}^*, H_{2(1)}^*)$, where

$$\begin{aligned}\frac{dC}{dt} &= \mu_1(G)C - \phi C \\ \frac{dB}{dt} &= 0\end{aligned}$$

$$\begin{aligned}
\frac{dA}{dt} &= 0 \\
\frac{dG}{dt} &= \phi G_{in} - \frac{\mu_1}{Y_{11}}C - \phi G \\
\frac{dE}{dt} &= \alpha_{12}\mu_1 C - \phi E \\
\frac{dF}{dt} &= \alpha_{13}\mu_1 C - \phi F \\
\frac{dCO_2}{dt} &= -\phi CO_2 \\
\frac{dH_2}{dt} &= \alpha_{15}\mu_1 C - \phi H_2
\end{aligned}$$

Setting each expression equal to zero, we get that $\mu_1 = \phi$, $G = G_{in} - \frac{C}{Y_{11}}$, $E = C\alpha_{12}$, $F = C\alpha_{13}$, $CO_2 = 0$, and $H_2 = C\alpha_{15}$. Additionally, from the $\mu_1 = \phi$ statement, we get that

$$G = \frac{\phi K_{11}}{\mu_{max1} - \phi}.$$

Therefore, our set of equilibrium points are

$$\left(C^*, 0, 0, \frac{\phi K_{11}}{\mu_{max1} - \phi}, C^* \alpha_{12}, C^* \alpha_{13}, 0, C^* \alpha_{15} \right),$$

where

$$C^* = Y_{11}G_{in} - Y_{11}\frac{\phi K_{11}}{\mu_{max1} - \phi}.$$

3. $E_3 = (0, B_3^*, 0, G_3^*, E_3^*, F_3^*, CO_{2(3)}^*, H_{2(3)}^*)$, where

$$\begin{aligned}
\frac{dC}{dt} &= 0 \\
\frac{dB}{dt} &= \mu_2 B - \phi B \\
\frac{dA}{dt} &= 0 \\
\frac{dG}{dt} &= \phi G_{in} - \frac{\mu_2}{Y_{21}}B - \phi G \\
\frac{dE}{dt} &= -\frac{\mu_{max2}}{Y_{22}}w_{22}\frac{G}{K_{21} + G}\frac{E}{K_{22} + E}B - \phi E
\end{aligned}$$

$$\begin{aligned}
\frac{dF}{dt} &= -\phi F \\
\frac{dCO_2}{dt} &= \alpha_{24}\mu_2 B - \phi CO_2 \\
\frac{dH_2}{dt} &= -\frac{\mu_{max2}}{Y_{25}} w_{25} \frac{G}{K_{21} + G} \frac{H_2}{K_{25} + H_2} B - \phi H_2
\end{aligned}$$

Setting each expression equal to zero, we get that $\mu_2 = \phi$, $B = Y_{21}(G_{in} - G)$, $E = 0$, $F = 0$, $CO_2 = \alpha_{24}B$, and $H_2 = 0$. From the fact that $\mu_2 = \phi$, we get that

$$G = \frac{\phi K_{21}}{\mu_{max2} - \phi}.$$

Then, we can find B and CO_2 . Thus, our set of equilibrium points are

$$\left(0, Y_{21} \left(G_{in} - \frac{\phi K_{21}}{\mu_{max2} - \phi}\right), 0, \frac{\phi K_{21}}{\mu_{max2} - \phi}, 0, 0, \alpha_{24} Y_{21} \left(G_{in} - \frac{\phi K_{21}}{\mu_{max2} - \phi}\right)\right)$$

4. $E_4 = (0, 0, A_4^*, G_4^*, E_4^*, F_4^*, CO_{2(4)}^*, H_{2(4)}^*)$, where

$$\begin{aligned}
\frac{dC}{dt} &= 0 \\
\frac{dB}{dt} &= 0 \\
\frac{dA}{dt} &= \mu_3 A - \phi A \\
\frac{dG}{dt} &= \phi G_{in} - \frac{\mu_3}{Y_{31}} A - \phi G \\
\frac{dE}{dt} &= \alpha_{32}\mu_3 A - \phi E \\
\frac{dF}{dt} &= -\frac{\mu_{max3}}{Y_{33}} w_{33} \frac{G}{K_{31} + G} \frac{F}{K_{33} + F} - \phi F \\
\frac{dCO_2}{dt} &= -\frac{\mu_{max3}}{Y_{34}} w_{33} \frac{G}{K_{31} + G} \frac{CO_2}{K_{34} + CO_2} - \phi CO_2 \\
\frac{dH_2}{dt} &= -\frac{\mu_{max3}}{Y_{35}} w_{33} \frac{G}{K_{31} + G} \frac{H_2}{K_{35} + H_2} A - \phi H_2
\end{aligned}$$

Setting each expression equal to zero, we get that $\mu_3 = \phi$, $G = G_{in} - \frac{A}{Y_{31}}$, $A = \frac{E}{\alpha_{32}}$, $F = 0$, $CO_2 = 0$, and $H_2 = 0$.

Then, from $\frac{dF}{dt} = 0$, we get that

$$-\frac{\mu_{max3}}{Y_{33}}w_{33}\frac{G}{K_{31} + G}\frac{1}{K_{34}} = \phi,$$

and

$$G = \frac{\phi K_{31} Y_{33} K_{34}}{-\mu_{max3} w_{33} - \phi Y_{33} K_{34}}$$

. Then, $A = -Y_{31}G + Y_{31}G_{in}$, and $E = \alpha_{32}A$. Thus, our set of equilibrium points are

$$(0, 0, -Y_{31}G^* + Y_{31}G_{in}, G^*, \alpha_{32}(-Y_{31}G^* + Y_{31}G_{in}), 0, 0, 0),$$

where

$$G^* = \frac{\phi K_{31} Y_{33} K_{34}}{-\mu_{max3} w_{33} - \phi Y_{33} K_{34}}$$

5. Remaining Equilibrium Points. We acknowledge the existence of other equilibrium points:

$$E_5 = (C_5^*, B_5^*, 0, G_5^*, E_5^*, F_5^*, CO_{2(5)}^*, H_{2(5)}^*),$$

$$E_6 = (C_6^*, 0, A_6^*, G_6^*, E_6^*, F_6^*, CO_{2(6)}^*, H_{2(6)}^*),$$

$$E_7 = (0, B_7^*, A_7^*, G_7^*, E_7^*, F_7^*, CO_{2(7)}^*, H_{2(7)}^*),$$

$$E_8 = (C_8^*, B_8^*, A_8^*, G_8^*, E_8^*, F_8^*, CO_{2(8)}^*, H_{2(8)}^*).$$

Chapter 4

Discussion and Conclusions

In this paper, we have explored the world of the gut microbiome and its members as well as the various modeling approaches. We used the Rios Garza [1] metabolite-explicit ordinary differential equations model.

We introduced a new parameter, H_2 , and modeled its interactions with the existing microbes. We examined the differences between constant glucose intake and three types of time-dependent glucose intake functions.

Through extensive numerical experiments, we observed that glucose intake is a vital aspect of this model. Even as a constant, the survival of all eight biomasses often completely changed when the G_{in} term was modulated. Often, to ensure the coexistence of all microbes, it was necessary to find an appropriate G_{in} term relative to the flow rate and initial conditions that balanced the model. If the constant was too high, all of the microbes would die, besides glucose. If the constant was too low, all of the microbes would also die, besides glucose. This phenomenon is observable in Figure 3.5, where a higher G_{in} term leads to lower biomasses for all other parameters, but the lower G_{in} causes the other biomasses to thrive.

We hope that this work will function as a means to further understand the health of the human gut, eliminating the difficulty of analysis for researchers.

Bibliography

- [1] D. Rios Garza, D. Gonze, H. Zafeiropoulos, B. Liu, and K. Faust, “Metabolic models of human gut microbiota: Advances and challenges,” *Cell Systems*, vol. 14, no. 2, pp. 109–121, Feb. 2023, ISSN: 24054712. DOI: 10.1016/j.cels.2022.11.002. Accessed: Dec. 2, 2025. [Online]. Available: <https://linkinghub.elsevier.com/retrieve/pii/S2405471222004379>.
- [2] E. Dempsey and S. C. Corr, “Lactobacillus spp. for Gastrointestinal Health: Current and Future Perspectives,” *Frontiers in Immunology*, vol. 13, p. 840245, Apr. 2022, ISSN: 1664-3224. DOI: 10.3389/fimmu.2022.840245. Accessed: Mar. 21, 2026. [Online]. Available: <https://www.frontiersin.org/articles/10.3389/fimmu.2022.840245/full>.
- [3] E. Lange, L. Kranert, J. Krüger, D. Benndorf, and R. Heyer, “Microbiome modeling: A beginner’s guide,” *Frontiers in Microbiology*, vol. 15, p. 1368377, Jun. 2024, ISSN: 1664-302X. DOI: 10.3389/fmicb.2024.1368377. Accessed: Aug. 27, 2025. [Online]. Available: <https://www.frontiersin.org/articles/10.3389/fmicb.2024.1368377/full>.
- [4] O. S. Venturelli et al., “Deciphering microbial interactions in synthetic human gut microbiome communities,” en, *Molecular Systems Biology*, vol. 14, no. 6, e8157, Jun. 2018, ISSN: 1744-4292, 1744-4292. DOI: 10.15252/msb.20178157. Accessed: Aug. 29, 2025. [Online]. Available: <https://www.embopress.org/doi/10.15252/msb.20178157>.
- [5] H. Wang, C.-X. Wei, L. Min, and L.-Y. Zhu, “Good or bad: Gut bacteria in human health and diseases,” *Biotechnology & Biotechnological Equipment*, vol. 32, no. 5, pp. 1075–1080, Jun. 11, 2018. DOI: 10.1080/13102818.2018.1481350.

- [6] A. S. Moorthy, S. P. J. Brooks, M. Kalmokoff, and H. J. Eberl, “A Spatially Continuous Model of Carbohydrate Digestion and Transport Processes in the Colon,” en, *PLOS ONE*, vol. 10, no. 12, P. E. Larsen, Ed., e0145309, Dec. 2015, ISSN: 1932-6203. DOI: 10.1371/journal.pone.0145309. Accessed: Sep. 8, 2025. [Online]. Available: <https://dx.plos.org/10.1371/journal.pone.0145309>.
- [7] H. Kettle, P. Louis, and H. J. Flint, “Process-based modelling of microbial community dynamics in the human colon,” en, *Journal of The Royal Society Interface*, vol. 19, no. 195, p. 20220489, Oct. 2022, ISSN: 1742-5662. DOI: 10.1098/rsif.2022.0489. Accessed: Aug. 27, 2025. [Online]. Available: <https://royalsocietypublishing.org/doi/10.1098/rsif.2022.0489>.
- [8] S. E. Power, P. W. O’Toole, C. Stanton, R. P. Ross, and G. F. Fitzgerald, “Intestinal microbiota, diet and health,” en, *British Journal of Nutrition*, vol. 111, no. 3, pp. 387–402, Feb. 2014, ISSN: 0007-1145, 1475-2662. DOI: 10.1017/S0007114513002560. Accessed: Mar. 16, 2026. [Online]. Available: https://www.cambridge.org/core/product/identifier/S0007114513002560/type/journal_article.
- [9] C. Long-Smith, K. J. O’Riordan, G. Clarke, C. Stanton, T. G. Dinan, and J. F. Cryan, “Microbiota-gut-brain axis: New therapeutic opportunities,” *Annual Review of Pharmacology and Toxicology*, vol. 60, no. 1, pp. 477–502, Jan. 6, 2020, ISSN: 0362-1642, 1545-4304. DOI: 10.1146/annurev-pharmtox-010919-023628. Accessed: Mar. 4, 2026. [Online]. Available: <https://www.annualreviews.org/doi/10.1146/annurev-pharmtox-010919-023628>.
- [10] A. M. Motelica-Wagenaar, A. Nauta, E. G. Van Den Heuvel, and R. Kleerebezem, “Flux analysis of the human proximal colon using anaerobic digestion model 1,” *Anaerobe*, vol. 28, pp. 137–148, Aug. 2014, ISSN: 10759964. DOI: 10.1016/j.anaerobe.2014.05.008. Accessed: Sep. 30, 2025. [Online]. Available: <https://linkinghub.elsevier.com/retrieve/pii/S1075996414000584>.

- [11] Y.-J. Zhang, S. Li, and R.-Y. Gan, “Impacts of gut bacteria on human health and diseases,” *International Journal of Molecular Sciences*, vol. 16, no. 4, pp. 7493–7519, Apr. 2, 2015. DOI: 10.3390/ijms16047493.
- [12] J. D. Lewis et al., “Incidence, Prevalence, and Racial and Ethnic Distribution of Inflammatory Bowel Disease in the United States,” en, *Gastroenterology*, vol. 165, no. 5, 1197–1205.e2, Nov. 2023, ISSN: 00165085. DOI: 10.1053/j.gastro.2023.07.003. Accessed: Mar. 19, 2026. [Online]. Available: <https://linkinghub.elsevier.com/retrieve/pii/S0016508523047765>.
- [13] K. Winglee et al., “Recent urbanization in China is correlated with a Westernized microbiome encoding increased virulence and antibiotic resistance genes,” en, *Microbiome*, vol. 5, no. 1, p. 121, Dec. 2017, ISSN: 2049-2618. DOI: 10.1186/s40168-017-0338-7. Accessed: Mar. 19, 2026. [Online]. Available: <https://microbiomejournal.biomedcentral.com/articles/10.1186/s40168-017-0338-7>.
- [14] M. Roberfroid, *PREBIOTICS*, in *Encyclopedia of Food Sciences and Nutrition (Second Edition)*, B. Caballero, Ed., Academic Press, 2003, pp. 4719–4723, ISBN: 978-0-12-227055-0.
- [15] S. Labarthe, B. Polizzi, T. Phan, T. Goudon, M. Ribot, and B. Laroche, “A mathematical model to investigate the key drivers of the biogeography of the colon microbiota,” *Journal of Theoretical Biology*, vol. 462, pp. 552–581, Feb. 2019, ISSN: 00225193. DOI: 10.1016/j.jtbi.2018.12.009. Accessed: Sep. 16, 2025. [Online]. Available: <https://linkinghub.elsevier.com/retrieve/pii/S002251931830599X>.
- [16] K. Hou et al., “Microbiota in health and diseases,” *Signal Transduction and Targeted Therapy*, vol. 7, no. 1, p. 135, Apr. 23, 2022, ISSN: 2059-3635. DOI: 10.1038/s41392-022-00974-4. Accessed: Oct. 8, 2025. [Online]. Available: <https://www.nature.com/articles/s41392-022-00974-4>.

- [17] R. Havenaar, “Intestinal health functions of colonic microbial metabolites: A review,” *Beneficial Microbes*, vol. 2, no. 2, pp. 103–114, Jun. 1, 2011, ISSN: 1876-2883, 1876-2891. DOI: 10.3920/BM2011.0003. Accessed: Feb. 10, 2026. [Online]. Available: https://brill.com/view/journals/bm/2/2/article-p103_103.xml.
- [18] X. Fu, Z. Liu, C. Zhu, H. Mou, and Q. Kong, “Nondigestible carbohydrates, butyrate, and butyrate-producing bacteria,” *Critical Reviews in Food Science and Nutrition*, vol. 59, S130–S152, sup1 Jun. 27, 2019, ISSN: 1040-8398, 1549-7852. DOI: 10.1080/10408398.2018.1542587. Accessed: Oct. 21, 2025. [Online]. Available: <https://www.tandfonline.com/doi/full/10.1080/10408398.2018.1542587>.
- [19] M. Roberfroid et al., “Prebiotic effects: Metabolic and health benefits,” en, *British Journal of Nutrition*, vol. 104, no. S2, S1–S63, Aug. 2010, ISSN: 0007-1145, 1475-2662. DOI: 10.1017/S0007114510003363. Accessed: Mar. 21, 2026. [Online]. Available: https://www.cambridge.org/core/product/identifier/S0007114510003363/type/journal_article.
- [20] P. D. Cani and N. M. Delzenne, “The gut microbiome as therapeutic target,” en, *Pharmacology & Therapeutics*, vol. 130, no. 2, pp. 202–212, May 2011, ISSN: 01637258. DOI: 10.1016/j.pharmthera.2011.01.012. Accessed: Mar. 21, 2026. [Online]. Available: <https://linkinghub.elsevier.com/retrieve/pii/S0163725811000362>.
- [21] M.-H. Lee, “Harness the functions of gut microbiome in tumorigenesis for cancer treatment,” en, *Cancer Communications*, vol. 41, no. 10, pp. 937–967, Oct. 2021, ISSN: 2523-3548. DOI: 10.1002/cac2.12200. Accessed: Mar. 21, 2026. [Online]. Available: <https://spj.science.org/doi/10.1002/cac2.12200>.
- [22] E. M. Schott et al., “Targeting the gut microbiome to treat the osteoarthritis of obesity,” en, *JCI Insight*, vol. 3, no. 8, e95997, Apr. 2018, ISSN: 2379-3708. DOI: 10.1172/jci.insight.95997. Accessed: Mar. 21, 2026. [Online]. Available: <https://insight.jci.org/articles/view/95997>.

- [23] Z. Jie et al., “The gut microbiome in atherosclerotic cardiovascular disease,” en, *Nature Communications*, vol. 8, no. 1, p. 845, Oct. 2017, ISSN: 2041-1723. DOI: 10.1038/s41467-017-00900-1. Accessed: Mar. 21, 2026. [Online]. Available: <https://www.nature.com/articles/s41467-017-00900-1>.
- [24] J. F. Cryan et al., “The microbiota-gut-brain axis,” *Physiological Reviews*, vol. 99, no. 4, pp. 1877–2013, 2019, PMID: 31460832. DOI: 10.1152/physrev.00018.2018. eprint: <https://doi.org/10.1152/physrev.00018.2018>. [Online]. Available: <https://doi.org/10.1152/physrev.00018.2018>.
- [25] S. Davari, S. Talaei, H. Alaei, and M. Salami, “Probiotics treatment improves diabetes-induced impairment of synaptic activity and cognitive function: Behavioral and electrophysiological proofs for microbiome–gut–brain axis,” *Neuroscience*, vol. 240, pp. 287–296, Jun. 2013, ISSN: 03064522. DOI: 10.1016/j.neuroscience.2013.02.055. Accessed: Mar. 4, 2026. [Online]. Available: <https://linkinghub.elsevier.com/retrieve/pii/S0306452213001966>.
- [26] R. D. Heijtz et al., “Normal gut microbiota modulates brain development and behavior,” *Proceedings of the National Academy of Sciences*, vol. 108, no. 7, pp. 3047–3052, Feb. 15, 2011, ISSN: 0027-8424, 1091-6490. DOI: 10.1073/pnas.1010529108. Accessed: Mar. 4, 2026. [Online]. Available: <https://pnas.org/doi/full/10.1073/pnas.1010529108>.
- [27] J. Cummings and G. Macfarlane, “The control and consequences of bacterial fermentation in the human colon,” *Journal of Applied Bacteriology*, vol. 70, no. 6, pp. 443–459, Jun. 1991, ISSN: 0021-8847. DOI: 10.1111/j.1365-2672.1991.tb02739.x. Accessed: Sep. 30, 2025. [Online]. Available: <https://sfamjournals.onlinelibrary.wiley.com/doi/10.1111/j.1365-2672.1991.tb02739.x>.

- [28] J. Daintith and E. A. Martin, Eds., *A dictionary of science* (Oxford paperback reference), 6th ed. Oxford ; New York: Oxford University Press, 2010, ISBN: 978-0-19-956146-9.
- [29] N. K. Leeuwendaal, C. Stanton, P. W. O’Toole, and T. P. Beresford, “Fermented foods, health and the gut microbiome,” *Nutrients*, vol. 14, no. 7, p. 1527, Apr. 6, 2022, ISSN: 2072-6643. DOI: 10.3390/nu14071527. Accessed: Oct. 18, 2025. [Online]. Available: <https://www.mdpi.com/2072-6643/14/7/1527>.
- [30] E. Beards, K. Tuohy, and G. Gibson, “Bacterial, SCFA and gas profiles of a range of food ingredients following in vitro fermentation by human colonic microbiota,” *Anaerobe*, vol. 16, no. 4, pp. 420–425, Aug. 2010, ISSN: 10759964. DOI: 10.1016/j.anaerobe.2010.05.006. Accessed: Sep. 30, 2025. [Online]. Available: <https://linkinghub.elsevier.com/retrieve/pii/S1075996410000934>.
- [31] I. Mukhopadhyaya and P. Louis, “Gut microbiota-derived short-chain fatty acids and their role in human health and disease,” *Nature Reviews Microbiology*, vol. 23, no. 10, pp. 635–651, Oct. 2025, ISSN: 1740-1526, 1740-1534. DOI: 10.1038/s41579-025-01183-w. Accessed: Feb. 9, 2026. [Online]. Available: <https://www.nature.com/articles/s41579-025-01183-w>.
- [32] M. A. Adrian, B. P. Ayati, and A. K. Mangalam, “A mathematical model of *Bacteroides thetaiotaomicron*, *Methanobrevibacter smithii*, and *Eubacterium rectale* interactions in the human gut,” en, *Scientific Reports*, vol. 13, no. 1, p. 21192, Dec. 2023, ISSN: 2045-2322. DOI: 10.1038/s41598-023-48524-4. Accessed: Aug. 27, 2025. [Online]. Available: <https://www.nature.com/articles/s41598-023-48524-4>.
- [33] M. Kumar, B. Ji, K. Zengler, and J. Nielsen, “Modelling approaches for studying the microbiome,” en, *Nature Microbiology*, vol. 4, no. 8, pp. 1253–1267, Jul. 2019, ISSN: 2058-5276. DOI: 10.1038/s41564-019-0491-9. Accessed: Aug. 29, 2025. [Online]. Available: <https://www.nature.com/articles/s41564-019-0491-9>.

- [34] H. Kettle, P. Louis, G. Holtrop, S. H. Duncan, and H. J. Flint, “Modelling the emergent dynamics and major metabolites of the human colonic microbiota,” en, *Environmental Microbiology*, vol. 17, no. 5, pp. 1615–1630, May 2015, ISSN: 1462-2912, 1462-2920. DOI: 10.1111/1462-2920.12599. Accessed: Sep. 8, 2025. [Online]. Available: <https://sfamjournals.onlinelibrary.wiley.com/doi/10.1111/1462-2920.12599>.
- [35] N. W. Smith, P. R. Shorten, E. Altermann, N. C. Roy, and W. C. McNabb, “Examination of hydrogen cross-feeders using a colonic microbiota model,” *BMC Bioinformatics*, vol. 22, no. 1, p. 3, Dec. 2021, ISSN: 1471-2105. DOI: 10.1186/s12859-020-03923-6. Accessed: Sep. 16, 2025. [Online]. Available: <https://bmcbioinformatics.biomedcentral.com/articles/10.1186/s12859-020-03923-6>.
- [36] S. Shibasaki and S. Mitri, “A spatially structured mathematical model of the gut microbiome reveals factors that increase community stability,” en, *iScience*, vol. 26, no. 9, p. 107499, Sep. 2023, ISSN: 25890042. DOI: 10.1016/j.isci.2023.107499. Accessed: Aug. 30, 2025. [Online]. Available: <https://linkinghub.elsevier.com/retrieve/pii/S2589004223015766>.
- [37] A. Budithi, S. Su, A. Kirshtein, and L. Shahriyari, “Data driven mathematical model of FOLFIRI treatment for colon cancer,” *Cancers*, vol. 13, no. 11, p. 2632, May 27, 2021, ISSN: 2072-6694. DOI: 10.3390/cancers13112632. Accessed: Sep. 30, 2025. [Online]. Available: <https://www.mdpi.com/2072-6694/13/11/2632>.
- [38] J. Cremer, M. Arnoldini, and T. Hwa, “Effect of water flow and chemical environment on microbiota growth and composition in the human colon,” en, *Proceedings of the National Academy of Sciences*, vol. 114, no. 25, pp. 6438–6443, Jun. 2017, ISSN: 0027-8424, 1091-6490. DOI: 10.1073/pnas.1619598114. Accessed: Sep. 8, 2025. [Online]. Available: <https://pnas.org/doi/full/10.1073/pnas.1619598114>.
- [39] V. Bucci and J. B. Xavier, “Towards Predictive Models of the Human Gut Microbiome,” en, *Journal of Molecular Biology*, vol. 426, no. 23, pp. 3907–3916, Nov. 2014, ISSN:

00222836. DOI: 10.1016/j.jmb.2014.03.017. Accessed: Aug. 27, 2025. [Online]. Available: <https://linkinghub.elsevier.com/retrieve/pii/S0022283614001788>.
- [40] S. Q. Fernandes and M. V. Kothare, *A Compartmental Model for Simulating the Gut-Brain Axis in Gastric Function Regulation*, en, Jun. 2025. DOI: 10.1101/2025.06.19.660643. Accessed: Mar. 5, 2026. [Online]. Available: <http://biorxiv.org/lookup/doi/10.1101/2025.06.19.660643>.
- [41] S. Shoaie and J. Nielsen, “Elucidating the interactions between the human gut microbiota and its host through metabolic modeling,” *Frontiers in Genetics*, vol. 5, Apr. 2014, ISSN: 1664-8021. DOI: 10.3389/fgene.2014.00086. Accessed: Aug. 28, 2025. [Online]. Available: <http://journal.frontiersin.org/article/10.3389/fgene.2014.00086/abstract>.
- [42] R. Muñoz-Tamayo, B. Laroche, É. Walter, J. Doré, and M. Leclerc, “Mathematical modelling of carbohydrate degradation by human colonic microbiota,” en, *Journal of Theoretical Biology*, vol. 266, no. 1, pp. 189–201, Sep. 2010, ISSN: 00225193. DOI: 10.1016/j.jtbi.2010.05.040. Accessed: Sep. 8, 2025. [Online]. Available: <https://linkinghub.elsevier.com/retrieve/pii/S0022519310002845>.
- [43] T. P. N. Bui, H. A. Schols, M. Jonathan, A. J. M. Stams, W. M. De Vos, and C. M. Plugge, “Mutual metabolic interactions in co-cultures of the intestinal anaerostipes rhamnosivorans with an acetogen, methanogen, or pectin-degrader affecting butyrate production,” *Frontiers in Microbiology*, vol. 10, p. 2449, Nov. 1, 2019, ISSN: 1664-302X. DOI: 10.3389/fmicb.2019.02449. Accessed: Feb. 13, 2026. [Online]. Available: <https://www.frontiersin.org/article/10.3389/fmicb.2019.02449/full>.
- [44] K. Schuchmann and V. Müller, “Energetics and application of heterotrophy in acetogenic bacteria,” *Applied and Environmental Microbiology*, vol. 82, no. 14, A. J. M. Stams, Ed., pp. 4056–4069, Jul. 15, 2016, ISSN: 0099-2240, 1098-5336. DOI: 10.1128/

- AEM.00882-16. Accessed: Feb. 16, 2026. [Online]. Available: <https://journals.asm.org/doi/10.1128/AEM.00882-16>.
- [45] D. Ríos-Covián, P. Ruas-Madiedo, A. Margolles, M. Gueimonde, C. G. De Los Reyes-Gavilán, and N. Salazar, “Intestinal short chain fatty acids and their link with diet and human health,” *Frontiers in Microbiology*, vol. 7, Feb. 17, 2016, ISSN: 1664-302X. DOI: 10.3389/fmicb.2016.00185. Accessed: Nov. 3, 2025. [Online]. Available: <http://journal.frontiersin.org/Article/10.3389/fmicb.2016.00185/abstract>.
- [46] E. Mutuyemungu, M. Singh, S. Liu, and D. J. Rose, “Intestinal gas production by the gut microbiota: A review,” *Journal of Functional Foods*, vol. 100, p. 105367, Jan. 2023, ISSN: 17564646. DOI: 10.1016/j.jff.2022.105367. Accessed: Feb. 16, 2026. [Online]. Available: <https://linkinghub.elsevier.com/retrieve/pii/S1756464622004376>.
- [47] A. Campbell, K. Gdanetz, A. W. Schmidt, and T. M. Schmidt, “H₂ generated by fermentation in the human gut microbiome influences metabolism and competitive fitness of gut butyrate producers,” *Microbiome*, vol. 11, no. 1, p. 133, Jun. 15, 2023, ISSN: 2049-2618. DOI: 10.1186/s40168-023-01565-3. Accessed: Nov. 5, 2025. [Online]. Available: <https://microbiomejournal.biomedcentral.com/articles/10.1186/s40168-023-01565-3>.
- [48] D. J. Morrison and T. Preston, “Formation of short chain fatty acids by the gut microbiota and their impact on human metabolism,” *Gut Microbes*, vol. 7, no. 3, pp. 189–200, May 3, 2016, ISSN: 1949-0984. DOI: 10.1080/19490976.2015.1134082.
- [49] D. Ternes et al., “The gut microbial metabolite formate exacerbates colorectal cancer progression,” en, *Nature Metabolism*, vol. 4, no. 4, pp. 458–475, Apr. 2022, ISSN: 2522-5812. DOI: 10.1038/s42255-022-00558-0. Accessed: Mar. 5, 2026. [Online]. Available: <https://www.nature.com/articles/s42255-022-00558-0>.
- [50] B. Momeni, L. Xie, and W. Shou, “Lotka-Volterra pairwise modeling fails to capture diverse pairwise microbial interactions,” en, *eLife*, vol. 6, e25051, Mar. 2017, ISSN:

- 2050-084X. DOI: 10.7554/eLife.25051. Accessed: Aug. 28, 2025. [Online]. Available: <https://elifesciences.org/articles/25051>.
- [51] M. E. Coleman, D. W. Dreesen, and R. G. Wiegert, “A simulation of microbial competition in the human colonic ecosystem,” en, *Applied and Environmental Microbiology*, vol. 62, no. 10, pp. 3632–3639, Oct. 1996, ISSN: 0099-2240, 1098-5336. DOI: 10.1128/aem.62.10.3632-3639.1996. Accessed: Sep. 30, 2025. [Online]. Available: <https://journals.asm.org/doi/10.1128/aem.62.10.3632-3639.1996>.
- [52] K. Faust et al., “Microbial Co-occurrence Relationships in the Human Microbiome,” en, *PLoS Computational Biology*, vol. 8, no. 7, C. A. Ouzounis, Ed., e1002606, Jul. 2012, ISSN: 1553-7358. DOI: 10.1371/journal.pcbi.1002606. Accessed: Mar. 9, 2026. [Online]. Available: <https://dx.plos.org/10.1371/journal.pcbi.1002606>.
- [53] R. R. Stein et al., “Ecological Modeling from Time-Series Inference: Insight into Dynamics and Stability of Intestinal Microbiota,” en, *PLoS Computational Biology*, vol. 9, no. 12, C. Von Mering, Ed., e1003388, Dec. 2013, ISSN: 1553-7358. DOI: 10.1371/journal.pcbi.1003388. Accessed: Aug. 28, 2025. [Online]. Available: <https://dx.plos.org/10.1371/journal.pcbi.1003388>.
- [54] H.-S. Song, W. Cannon, A. Beliaev, and A. Konopka, “Mathematical Modeling of Microbial Community Dynamics: A Methodological Review,” en, *Processes*, vol. 2, no. 4, pp. 711–752, Oct. 2014, ISSN: 2227-9717. DOI: 10.3390/pr2040711. Accessed: Mar. 10, 2026. [Online]. Available: <https://www.mdpi.com/2227-9717/2/4/711>.
- [55] M. Wade et al., “Perspectives in mathematical modelling for microbial ecology,” en, *Ecological Modelling*, vol. 321, pp. 64–74, Feb. 2016, ISSN: 03043800. DOI: 10.1016/j.ecolmodel.2015.11.002. Accessed: Mar. 5, 2026. [Online]. Available: <https://linkinghub.elsevier.com/retrieve/pii/S0304380015005190>.
- [56] P. De Jong, M. M. M. Vissers, R. Van Der Meer, and I. M. J. Bovee-Oudenhoven, “In Silico Model as a Tool for Interpretation of Intestinal Infection Studies,” en, *Applied and*

- Environmental Microbiology*, vol. 73, no. 2, pp. 508–515, Jan. 2007, ISSN: 0099-2240, 1098-5336. DOI: 10.1128/AEM.01299-06. Accessed: Oct. 1, 2025. [Online]. Available: <https://journals.asm.org/doi/10.1128/AEM.01299-06>.
- [57] C. Williams, G. Walton, L. Jiang, S. Plummer, I. Garaiova, and G. Gibson, “Comparative Analysis of Intestinal Tract Models,” en, *Annual Review of Food Science and Technology*, vol. 6, no. 1, pp. 329–350, Apr. 2015, ISSN: 1941-1413, 1941-1421. DOI: 10.1146/annurev-food-022814-015429. Accessed: Sep. 30, 2025. [Online]. Available: <https://www.annualreviews.org/doi/10.1146/annurev-food-022814-015429>.
- [58] E. Ferrannini, “Physiology of Glucose Homeostasis and Insulin Therapy in Type 1 and Type 2 Diabetes,” en, *Endocrinology and Metabolism Clinics of North America*, vol. 41, no. 1, pp. 25–39, Mar. 2012, ISSN: 08898529. DOI: 10.1016/j.ec1.2012.01.003. Accessed: Mar. 25, 2026. [Online]. Available: <https://linkinghub.elsevier.com/retrieve/pii/S0889852912000047>.